Published in final edited form as:
Bioconjug Chem. 2010 August 18; 21(8): 1545–1553. doi:10.1021/bc100202y.

Synthesis and evaluation of new spacers for use as dsDNA endcaps

Pei-Sze Ng[†], **Brian M. Laing**[†,‡], **Ganesan Balasundarum**[†], **Maneesh Pingle**[†], **Alan Friedman**[§], and **Donald E. Bergstrom**[†,‡,*]

[†] Department of Medicinal Chemistry and Molecular Pharmacology, Purdue University, West Lafayette, IN 47907

[§] Department of Biological Sciences, Purdue University, West Lafayette, IN 47907

[‡] Bindley Bioscience Center, Purdue University, West Lafayette, IN 47907

Abstract

A series of aliphatic and aromatic spacer molecules designed to cap the ends of DNA duplexes have been synthesized. The spacers were converted into dimethoxytrityl protected phosphoramidites as synthons for oligonucleotides synthesis. The effect of the spacers on the stability of short DNA duplexes was assessed by melting temperature studies. Endcaps containing amide groups were found to be less stabilizing than the hexaethylene glycol spacer. Endcaps containing either a terthiophene or a naphthalene tetracarboxylic acid dimide were found to be significantly more stabilizing. The former showed a preference for stacking above an A•T base pair. Spacers containing only methylene (-CH_2-) and amide (-CONH-) groups interact weakly with DNA and consequently may be optimal for applications that require minimal influence on DNA structure but require a way to hold the ends of double-stranded DNA together.

Keywords

double-stranded DNA; spacer; phosphoramidite; thermal melting

Introduction

Short double-stranded DNA segments are required as components of DNA-protein complexes for crystallographic studies. However, it is often difficult to co-crystallize a protein with an oligonucleotide segment that constitutes the recognition/binding site. Among strategies that merit investigation as potentiators of co-crystallization is the use of short pre-organized DNA segments in crystallization experiments. One way to effectively pre-organize short oligonucleotides into a duplex structure is to covalently link the two complementary strands (1). It is well established that covalently attached linkers spanning the ends of complementary DNA strands significantly stabilize the duplex structure (2–10). This enhanced stabilization could be useful for increasing the pre-organization of DNA duplex fragments that are commonly involved in the recognition and binding of enzymes involved in degradation, repair, and synthesis of nucleic acids. We have previously shown

[*]Correspondence to: Donald Bergstrom, Department of Medicinal Chemistry and Molecular Pharmacology, Birck Nanotechnology Center, Purdue University, 1205 W State St, West Lafayette, IN 47907-2057, Telephone: (765) 494-6275; Fax: (765) 494-1414, bergstrom@purdue.edu.

Supporting Information Available: ^{1}H, ^{13}C and ^{31}P NMR spectra of synthesized compounds; Oligonucleotide MALDI-TOFMS characterization data. This material is available free of charge via the Internet at http://pubs.acs.org.

that DNA ‘endcapped’ at both ends by non-nucleotide linkers are useful for stabilizing short duplex sequences for studying the DNA footprint of T4 DNA ligase (11).

Ideally, the linker should be a molecule that would not alter the duplex in a way that would either hinder binding, or prevent readjustment of the structure as dictated by the binding protein. A linker that allows the protein to dictate the crystallization process would be preferable. Although there are a number of well-established linkers, particularly hexaethylene glycol, which is commercially available as a DMTr protected phosphoramidite, the family of stilbene linkers originally developed by Letsinger and coworkers (8,9) and the naphthalene and perylene based linkers reported by McLaughlin and coworkers (3,12), we thought it worthwhile to expand the potential repertoire of linkers. We were concerned that the hexaetheylene glycol spacer was neither sufficiently stabilizing nor useful for crystallographic studies because of its inherent disorder. A disadvantage of the stilbene linkers is that they are photosensitive. In addition, an X-ray structure of a duplex oligonucleotide capped by a stilbene linker has been obtained and it was found that stilbene has considerable influence on the crystallization because of its tendency to self-associate (13) and the perylene based linkers have been shown to self-associate to form dimerized hairpins (14). With these considerations in mind, we designed a set of very simple amide containing spacers, in which the total spacer length was close to the optimal 16–17 Å phosphate-oxygen to phosphate-oxygen distance required to span the ends of a duplex without distortion. The amide groups were expected to confer significantly more rigidity to the spacers than would be expected for hexaethylene glycol. Based on X-ray crystallographic studies of DNA polymerases, it is known that amide groups interact with the top face of a duplex base pair (15,16). This interaction appears to involve both a CH-π interaction (acidic α-H positioned in close proximity with the π-orbitals of a nucleobase) and stacking of an amide group, and may provide part of the driving force for the conformation switch between the open and closed form of the DNA polymerase (16). In the event that these interactions are significant, and realizing that one could not reasonably design a spacer with sufficiently precise orientation and positioning of the amide groups, we chose to make a series of amide containing spacers in which the amide positions vary (Figure 1). At the same time, the scope of the study was expanded by including hydrophobic spacers in order to weigh the influence of hydrophobicity on duplex stability in direct comparison to the more hydrophilic amide containing spacers. For these comparative studies we have adopted a very simple model system, a four base pair stem, for which T_m values fall in a range that can be readily measured, but for which differences in capping ability would be easily differentiated.

EXPERIMENTAL PROCEDURES

General Information

Reagents were purchased from Aldrich Chemical Company, Inc. (Milwaukee, WI) and were used as obtained unless otherwise stated. Anhydrous solvents used for synthesis were purchased in Sure-Seal containers or distilled from appropriate drying reagents. 2-Cyanoethyl tetraisopropylphosphorodiamidite and tetrazole were purchased from ChemGenes Corporation (Waltham, MA). Standard phosphoramidite monomers and other reagents for oligonucleotide synthesis were purchased from Glen Research Corp. (Sterling, VA). Thin-layer chromatography (TLC) was performed using Sigma-Aldrich TLC plates, silica gel on aluminum 60F-254 plates. Purification of compounds by silica gel chromatography was performed using Aldrich 230–400 mesh, 60 Å silica gel. Nuclear magnetic resonance spectra were obtained using 250, 300 or 500 MHz Bruker spectrometers. ^{1}H and ^{13}C spectra were referenced to TMS while ^{31}P spectra were referenced to an 85% phosphoric acid external standard.

Oligonucleotides (Figure 1) were synthesized on an Applied Biosystems 392 DNA/RNA synthesizer using standard phosphoramidite chemistry. Oligonucleotides were either purified by 20% polyacrylamide gel (PAGE, 60cm × 40cm × 0.15 cm) (trityl off) with 7 M urea in 1X Tris-borate-EDTA (TBE) buffer at a constant power of 60 watts or by HPLC (trityl on) on a Varian C18 Dynamax-100 60 Å column (7.9 mm × 250 mm) at a flow rate of 4 mL/min. Mobile phase A was 0.1M triethylammonium acetate (pH 7.0)/5% acetonitrile and Mobile phase B was 90% acetonitrile. The solvent program was a gradient starting at 100% A and linearly increasing to 45% B in 60 minutes. For analytical HPLC a Varian Microsorb-MV-100 Å (4.6 mm × 250 mm) column at a flow rate of 1 mL/min was used. The diode array detector was set at 260 nm. The oligonucleotides were desalted by 2-propanol precipitation or by elution using CH_3CN/H_20 (1:1) from C18 Sep-pak cartridges (Waters). The oligonucleotides were characterized by MALDI-TOFMS (Table S4–supplementary data)

Spacer Synthesis

The synthetic transformations are summarized in Scheme 1.

2-(*tert*-Butyldimethylsilyloxy)ethylamine (6)—To a solution of ethanolamine **(5)** (7.24 mL, 120 mmol, 1 equiv) in anhydrous CH_2Cl_2 (100 mL) at 0°C, were added anhydrous triethylamine (18.5 mL, 132 mmol, 1.1 equiv), *tert*-butyldimethylsilyl chloride (20.10 g, 132 mmol, 1.1 equiv) and a catalytic amount of 4-(*N*, *N*-dimethylamino)pyridine (DMAP) (0.5 g). The reaction mixture was stirred under argon overnight. The reaction was quenched with water (50 mL) and the layers separated. The organic layer was washed with water, brine, dried (Na_2SO_4), filtered and concentrated in vacuo to give colorless oil (17.96 g, 86%). ^{1}H NMR (250 MHz, $CDCl_3$, δ, ppm): 3.63 (t, 2H, J = 5.5Hz), 2.78 (t, 2H, J = 6 Hz), 0.81 (s, 9H), 0.06 (s, 6H). ^{13}C NMR (75 MHz, $CDCl_3$, δ, ppm): 65.16, 44.27, 25.90, 18.30, − 5.33. HRMS (EI, M-CH_3^+): calcd. for $C_7H_{18}NOSi$ 160.1158 act. 160.1165.

***N*,*N*′-Bis[2-(*tert*-butyldimethylsilyloxyethyl]-2,2′-oxydiacetamide (7)—**To a solution of **6** (16.26 g, 93 mmol, 2.2 equiv) in anhydrous CH_2Cl_2 (40mL) at 0° C, was added anhydrous triethylamine (17.8 mL, 127 mmol, 3 equiv) and diglycolyl chloride (5 mL, 42.5 mmol, 1 equiv.) was added dropwise with a syringe. The reaction mixture was stirred under argon overnight. The reaction was quenched with water (40 mL) and the layers separated. The organic layer was washed with 5% acetic acid (2 × 40 mL), 5% aqueous $NaHCO_3$ (2 × 40 mL), brine, dried (Na_2SO_4) and concentrated in vacuo to give a brown oil (14.75 g, 78 %). ^{1}H NMR (250 MHz, $CDCl_3$, δ, ppm): 4.07, (s, 4H), 3.71 (t, 4H, J= 5.6 Hz), 3.41–3.48 (t, 4H, J = 5.6 Hz), 0.090 (s, 18H), 0.076 (s, 9H). ^{13}C NMR (75 MHz, $CDCl_3$, δ, ppm): 168.14, 71.16, 61.58, 40.99, 25.78, 18.19, −5.42. HRMS (EI, M+H^+): calcd. for $C_{20}H_{45}N_2O_5Si_2$ 449.2867 act. 449.2849.

***N*,*N*′-Bis(2-hydroxyethyl)-2,2′-oxydiacetamide (8)—**To a solution of **7** (14.06 g, 31.3 mmol) in 95% ethanol (15 mL) was added 2.9 % w/w of conc. HCl in 95 % ethanol (15 mL). The reaction mixture was stirred under argon for 15 min and solvent removed in vacuo to give an orange solid. The orange solid was dissolved in methanol (20 mL), washed with hexane (3 × 30 mL), dried (Na_2SO_4) and concentrated in vacuo to give an orange solid (6.47 g, 94 %). ^{1}H NMR (250 MHz, $CDCl_3$, δ, ppm): 4.06 (s, 4H), 3.63 (t, 4H, J = 5.8 Hz), 3.34–3.39 (m, 4H). ^{13}C NMR (75 MHz, $CDCl_3$, δ, ppm): 172.00, 71.42, 61.44, 42.58. HRMS (EI, M-OH^+): calcd. for $C_8H_{15}N_2O_4$ 203.1032 act. 203.1034.

***N*-[2-(4, 4′-dimethoxytrityl)oxyethyl]-*N*′-(2-hydroxyethyl)-2,2′-oxydiacetamide (9)—**To a solution of **8** (2.00 g, 90.8 mmol, 1 equiv) in anhydrous pyridine (35 mL) at 0° C, was added 4, 4′-dimethoxytrityl chloride (3.23 g, 90.8 mmol, 1 equiv). The reaction mixture

was stirred under argon overnight. Upon completion as judged by TLC, pyridine was removed in vacuo. The crude brown product was dissolved in CH_2Cl_2 (40 mL), washed with aqueous 5 % $NaHCO_3$, brine and dried (Na_2SO_4). CH_2Cl_2 was removed in vacuo and the crude product purified by flash chromatography (silica gel, 0–5 % CH_3OH/1 % Et_3N/ CH_2Cl_2) to give a brown foam (1.67 g, 35.2 %). ^1H NMR (250 MHz, CD_2Cl_2, δ, ppm): 6.82–7.46 (m, 13H), 4.03 (s, 2H), 4.01 (s, 2H), 3.78 (s, 6H), 3.59 (m, 2H), 3.48 (m, 2H), 3.33 (m, 2H), 3.20 (m, 2H). ^{13}C NMR (75 MHz, CD_2Cl_2, δ, ppm): 169.81, 168.93, 158.98, 145.32, 136.31, 130.32, 128.34, 128.21, 127.22, 113.52, 86.53, 71.44, 62.52, 62.02, 55.61, 42.23, 39.54. HRMS (ESI, M+H^+): calcd. for $C_{29}H_{35}N_2O_7$ 523.2444 act. 523.2445.

***N*-[3-O-(2-cyanoethyl-*N*,*N*-diisopropylphosphoramidite)ethyl]-*N′*-[2-(4,4′–dimethoxytrityl)oxyethyl]-2,2′-oxydiacetamide (10)—**To a solution of **9** (211.2 mg, 0.404 mmol, 1 equiv) in anhydrous CH_2Cl_2 (5mL), were added anhydrous diisopropylethylamine (0.25mL, 1.45 mmol, 3.6 equiv) and 2-cyanoethyldiisopropyl chlorophosphoramidite (0.49 mL, 0.485 mmol, 1.2 equiv). The reaction was stirred for two hours at room temperature under argon. When the reaction was completed as judged by TLC, the reaction mixture was washed with aqueous 5% $NaHCO_3$, water and dried (Na_2SO_4). The crude product was further purified by flash chromatography (silica gel, 5: 4: 1 hexane/CH_2Cl_2/Et_3N to give a yellow oil (106.7 mg, 53.5 %). ^{31}P NMR (100.8 MHz, CD_2Cl_2, δ, ppm): 148.3 (referenced to external 85 % H_3PO_4).

***N*, *N′*-Bis-(4-hydroxybutanoyl)-1,3-propanediamine (18)—**1, 3-Diaminopropane (2.0 mL, 24 mmol), δ-butyrolactone **(17)** (6.2 mL, 80 mmol) and DMAP (40 mg, 0.32 mmol) in methanol (30 mL) was kept under reflux for overnight. The solvent was removed by rotary evaporation, CH_2Cl_2 (50mL) was added to the residue and with stirring on low heat to break up the white color solid. The solid was filtered and mixed with CH_2Cl_2 (50 mL) and again stirred at low heat and filtered. This procedure was repeated once more and the final white solid was dried under vacuum (4.6g, 80 %). ^1H NMR (250 MHz, DMSO-d_6, δ, ppm) 1.43–1.65 (m, 6H), 2.07 (t, J = 9 Hz, 4H), 2.99 (t, J= 6Hz, 2H), 3.01 (t, J = 6Hz, 2H), 3.34 (t, J =6Hz, 4H), 4.48 (s, 2H), 7.76 (t, J = 6 Hz, 2H); ^{13}C NMR (75 MHz, $CDCl_3$, δ, ppm) 29.01, 29.65, 32.52, 36.62, 60.67, 172.52. HRMS (ESI, M + H^+) calcd. for $C_{11}H_{22}N_2O_4$ 247.1657, found 247.1657.

***N*-{4-[4,4′-(Dimethoxytrityl)oxy]butanoyl}-*N′*-4-hydroxybutanoyl-1,3-propanediamine (19)—**Diol **18** (2.46g, 10 mmol) was co-evaporated with dry pyridine (3 × 20 mL), dissolved in dry pyridine (30 mL) and after cooling to 0° C in an ice bath, 4, 4′-dimethoxytrityl chloride (4.4g, 13 mmol) in CH_2Cl_2 (20mL) was added dropwise slowly. The flask was removed from ice and the reaction mixture was stirred overnight, quenched with methanol (1 mL), diluted with CH_2Cl_2 (200 mL), washed with 5% $NaHCO_3$ (2 × 200 mL), brine (100 mL) and dried over anhydrous sodium sulfate. The solution was concentrated in vacuo and the crude product was purified by silica gel chromatography in a gradient of methanol (0 to 5 %) in $CHCl_3$ containing 0.5 % Et_3N. The appropriate fractions were combined, evaporated and dried in vacuo to give compound **19** as pale yellow foam (2.9g, 53%), R_f 0.50 ($CHCl_3$-MeOH 9:1 v/v). ^1H NMR (250 MHz, $CDCl_3$, δ, ppm) 1.49–1.53 (m, 2H), 1.81–1.94 (m, 4H), 2.31 (t, J = 6Hz, 2H), 2.33 (t, J = 6Hz, 2H), 3.08–3.20 (m, 6H), 3.63 (t, J = 6Hz, 2H), 3.76 (s, 6H), 6.82 (d, J = 12.3, 4H), 7.18–7.32 (m, 7H), 7.39 (d, J = 9.0 Hz, 2H); ^{13}C NMR (62.5 MHz, $CDCl_3$, δ, ppm) 26.04, 28.18, 29.42, 33.70, 33.83, 35.75, 35.81, 55.11, 61.96, 62.32, 85.83, 112.96, 126.62, 127.68, 127.99, 129.86, 136.17, 144.94, 158.28, 173.76, 173.95. HRMS (ESI, M + Na^+) calcd. for $C_{32}H_{40}N_2O_6$ 571.2784, act. 571.2785.

***N*-[4-O-(2-cyanoethyl-*N*,*N*-diisopropylphophoramidite)butanoyl]-*N′*-{4-[4,4′-(dimethoxytrityl)oxy]butanoyl}-1,3-propanediamine (20)—**The mono-DMT-derivative **19** (0.55g, 1 mmol) was co-evaporated with 10 % dry pyridine in CH_2Cl_2 (3 × 10 mL), and DIEA (0.63 mL, 3.6 mmol) was added with stirring under nitrogen followed by the addition of 2-cyanoethyl diisopropylchlorophosphoramidite (0.27 mL, 1.2 mmol). The reaction was performed at room temperature for two hours with TLC monitoring. After reaction completion, the mixture was quenched with 4 drops of anhydrous methanol and CH_2Cl_2 (20 mL) was added. The methylene chloride solution was washed once with 5 % $NaHCO_3$ (20 mL), once with brine (10 mL) and then dried over anhydrous sodium sulfate. The solution was concentrated in vacuo and the crude product was purified by silica gel chromatography in a gradient of methanol (0 to 5 %) in CH_2Cl_2 containing 0.5% Et_3N. The appropriate fractions were combined, evaporated and dried under vacuum to give phosphoramidite **20** as pale yellow product (0.4 g, 54 %), R_f 0.90 (CH_2C_2-MeOH 9:1 v/v); HRMS (ESI, $M+H^+$) calcd. for $C_{41}H_{57}N_4O_7P$ 749.4043, found 749.4050; ^{31}P NMR (100.8 MHz, $CDCl_3$, ppm) δ 165.0 (referenced to external 0.0485M triphenylphosphate in $CDCl_3$).

***N*, *N′*-Bis-(5-hydroxypentanoyl)-1,3-propanediamine (22)—**1,3-Diaminopropane (1.7 mL, 20 mmol), δ-valerolactone (7.5 mL, 80 mmol) and DMAP (40 mg, 0.32 mmol) in methanol (30 mL) were refluxed overnight. The solvent was removed by rotary evaporation, CH_2Cl_2 (50 mL) was added to the residue with stirring on low heat to break up the white color solid. The solid was filtered and mixed with CH_2Cl_2 (50 mL) and again stirred at low heat and filtered. This procedure was repeated once more and the final white solid was dried under vacuum (4.65g, 85%). ^1H NMR (250 MHz, DMSO-d_6, δ, ppm) 1.31–1.54 (m, 10 H), 2.03 (t, J = 9 Hz, 4H), 2.99 (t, J = 6Hz, 2H), 3.01 (t, J =6 Hz, 2H), 3.33–3.38 (m, 4H), 4.35 (s, 2H), 7.74 (t, J = 3Hz, 2H); ^{13}C NMR (75 MHz, DMSO-d_6, δ, ppm) 22.30, 29.75, 32.42, 35.63, 36.60, 60.79, 172.45. HRMS (ESI, $M+H^+$) Calcd. for $C_{13}H_{26}N_2O_4$ 275.1970, act. 275.1972.

***N*-{5-[4,4′-(Dimethoxytrityl)oxy]pentanoyl}-*N′*-(5-hydroxypentanoyl]-1,3-propanediamine (23)—**Diol **22** (2.75g, 10 mmol) was co-evaporated with dry pyridine (3×20 mL), dissolved in dry pyridine (30 mL) and after cooling to 0° C in an ice bath, 4,4′ dimethoxytrityl chloride (4.4g, 13 mmol) in CH_2Cl_2 (20 mL) was added dropwise slowly. The flask was removed from ice and the reaction mixture was stirred overnight, quenched with methanol (1 mL), diluted with CH_2Cl_2 (200 mL), washed with 5 % $NaHCO_3$ (2 × 200 mL), brine (100 mL) and dried over anhydrous sodium sulfate. The solution was concentrated in vacuo and the crude product was purified by silica gel chromatography in a gradient of methanol (0 to 5%) in $CHCl_3$ containing 0.5% Et_3N. The appropriate fractions were combined, evaporated and dried in vacuum to give compound **23** as pale yellow foam (2.65g, 46%), R_f 0.5 ($CHCl_3$-MeOH 9:1 v/v); ^1H NMR (250 MHz, $CDCl_3$, δ, ppm) 1.54–1.72 (m, 10H), 2.12–2.24 (m, 4H), 3.06 (t, J = 6 Hz, 2H), 3.19 (t, J = 6Hz, 2H), 3.21 (t, J = 6Hz, 2H), 3.58 (t, J = 6Hz, 2H), 3.75 (s, 6H), 6.81 (d, J =6Hz, 4H), 7.17–7.32 (m, 7H), 7.40–7.43 (m, 2H); ^{13}C NMR (75 MHz, $CDCl_3$, δ, ppm) 22.01, 22.75, 29.61, 29.63, 31.98, 35.80, 35.89, 36.10, 36.47, 55.18, 61.78, 62.93, 76.75, 77.18, 77.60, 85.77, 112.99, 126.62, 127.71, 128.13, 129.98, 136.49, 145.23, 158.30, 173.92, 173.98. HRMS (ESI, $M+Na^+$) calcd. for $C_{34}H_{44}N_2O_6$ 599.3097, found 599.3106.

***N*-[5-O-(2-Cyanoethyl-*N*, *N*-diisopropylphosphoramidite)pentanoyl]-*N′*-{5-[4,4′-(dimethoxytrityl)oxy]pentanoyl}-1,3-propanediamine (24)—**The mono-DMT-derivative **23** (0.4g, 0.7 mmol) was co-evaporated with 10% dry pyridine in CH_2Cl_2 (3 × 10 mL), and DIEA (0.43 mL, 2.5 mmol) was added with stirring under nitrogen followed by the addition of 2-cyanoethyl diisopropylchlorophosphoramidite (0.19mL, 0.84 mmol). The reaction was performed at room temperature for two hours with TLC monitoring. After the

reaction completion, the mixture was quenched with 4 drops of anhydrous methanol, CH_2Cl_2 (20 mL) was added and the mixture was washed with 5 % $NaHCO_3$ (2 × 20 mL), brine (10 mL) and dried over anhydrous sodium sulfate. The solution was concentrated in vacuo and the crude product was purified by silica gel chromatography in a gradient of methanol (0 to 5%) in CH_2Cl_2 containing 0.5% Et_3N. The appropriate fractions were combined, evaporated and dried in vacuum to give phosphoramidite **24** as pale yellow product (0.3g, 55%), R_f 0.92 (CH_2Cl_2-MeOH 9:1 v/v); HRMS (ESI, M+Na^+) calcd. for $C_{43}H_{61}N_4O_7P$ 799.4175, found 799.4169; ^{31}P NMR (100.8 MHz, $CDCl_3$, δ, ppm) 164.5 (referenced to external 0.0485M triphenylpohosphate in $CDCl_3$).

Methyl 2-(2-(benzyloxy)ethoxy)acetate (26)—2-Benzyloxyethanol **(25)** (9.96 mL, 70 mmol) was added to a suspension of NaH (3.4 g, 84 mmol) in anhydrous THF (100 mL) under argon. The mixture was stirred for 1h at r.t. then cooled to 0 °C. Methyl bromoacetate (7.72 mL, 84 mmol) was added slowly and the mixture was allowed to react at room temperature for 16 h. The reaction was quenched with H_2O (30 mL) and the product extracted with ethyl acetate (5 × 50 mL). The ethyl acetate fractions were combined and washed successively with H_2O (3 × 100 mL) and brine (3 × 100 mL). The organic fraction was dried over anhyd $MgSO_4$ and concentrated in vacuo. The crude product was purified by silica gel chromatography (ethyl acetate-hexanes 1:4). The appropriate fractions were combined, evaporated and dried under vacuum to give **26** (13.2 g, 84%) as yellow oil. R_f 0.67 (ethyl acetate-hexanes 1:1 v/v). ^1H NMR (300 MHz, $CDCl_3$, δ, ppm): 7.28 (m, 5H), 4.56 (s, 2H), 4.18 (s, 2H), 3.80–3.68 (m, 7H). ^{13}C NMR (75 MHz, $CDCl_3$, δ, ppm): 170.8, 138.1, 128.3, 127.7, 73.2, 71, 69.5, 68.7. HRMS (EI, M^+) Calcd for $C_{12}H_{16}O_4$ 224.1049, act. 224.1045.

2-(2-(Benzyloxy)ethoxy)acetic acid (27)—26 (7 g, 29.38 mmol) was dissolved in 20 mL methanol and heated to ~ 35 °C with stirring. KOH (4.95 g, 88.13 mmol) was added. The mixture was stirred with TLC monitoring (1:1 ethyl acetate/hexanes) for 1 hr. The reaction was quenched by adding 80 mL H_2O. The unreacted ester was extracted with ether (2 × 50 mL). The aqueous portion was acidified to pH 2 with 6 N HCl then extracted with ether (3 × 50 mL) the ether layers were combined, dried over Na_2SO_4 and dried under vacuum to yield **27** (5.83g 95%) as a clear oil. ^1H NMR (300 MHz, DMSO-d_6, δ, ppm): 12.62 (s, 1H), 7.33 (m, 5H), 4.48 (s, 2H), 4.04 (s, 2H), 3.55–3.65 (m, 4H). ^{13}C NMR (75 MHz, DMSO-d_6, δ, ppm): 171.73, 138.48, 128.26, 127.56, 127.43, 72.07, 71.74, 69.89, 67.16, 60.31. HRMS (ESI, M + H^+) Calcd. for $C_{11}H_{15}O_4$ 211.0970, act. 211.0971.

***N*, *N′*-Bis-(2-(2-benzyloxyethoxy)ethanoyl)-1,3-propanediamine (28)—27** (2.13 g, 10.12 mmol) was dissolved in dry DMF (10 mL) under argon. TBTU (3.25 g, 10.12 mmol) and N-methylmorpholine (1.02 g, 10.12 mmol) was added and the mixture stirred for 15 mins. 1, 3-Diaminopropane (0.28 mL, 4.05 mmol) was dissolved in dry DMF (5 mL) and added slowly. The mixture was stirred overnight at room temperature. DMF was evaporated under reduced pressure and the residue was dissolved in ethyl acetate (100 mL), washed with 5% $NaHCO_3$ (75 mL × 2), 10 % CuSO4 (75 mL × 2), brine (75 mL). The organic layer was dried over anhyd magnesium sulfate and concentrated under vacuum. The crude product was purified by silica gel chromatography (0–5% MeOH/ethyl acetate). The appropriate fractions were combined evaporated and dried under vacuum to yield of **28** (0.92 g, 50 %) as a light brown oil R_f 0.68 (10% MeOH/ethyl acetate 9:1 v/v). ^1H NMR (300 MHz, DMSO-d_6, δ, ppm): 7.71 (t, J= 7 Hz, 2H), 7.30 (m, 10H), 4.49 (s, 4H), 3.86 (s, 4H), 3.61 (m, 8H), 3.03 (q, 4H, J = 7 Hz), 1.44 (t, 2H, J = 7 Hz). ^{13}C NMR (75 MHz, DMSO-d_6, δ, ppm): 169.17, 138.33, 128.23, 127.52, 72.11, 70.23, 70.01, 68.950, 35.50, 29.38. HRMS (ESI, M + H^+) Calcd. for $C_{25}H_{35}N_2O_6$ 459.2495, act. 459.2502.

***N*, *N′*-Bis-(2-(2-hydroxyethoxy)ethanoyl)-1,3-propanediamine (29)—28** (2.73 mg, 5.9 mmol) was dissolved in 40 mL EtOH. Pd/C (10% wt, 800 mg) was added and the mixture was treated with H_2 gas (55 psi) on a Parr apparatus for 12 H. The mixture was filtered over celite on a sintered glass funnel, evaporated and dried in vacuum to give compound **29** as a white solid (1.548g, 94%). ^{1}H NMR (300 MHz, DMSO –d_6, δ, ppm): 7.91 (s, 2H), 4.84 (s, 2H), 3.92 (s, 4H), 3.48 (m, 8H), 3.12 (m, 4H), 1.562 (m, 2H). ^{13}C NMR (75 MHz, DMSO-d_6, δ, ppm): 169.53, 72.91, 69.99, 60.13, 35.71, 29.44. HRMS (ESI, M + Na^+) calcd for $C_{11}H_{22}N_2NaO_6$ 301.1376, act. 301.1372.

***N*-(2-(2-(4, 4′-dimethoxytrityloxy)ethoxy)ethanoyl)-*N′*-(2-(2-hydroxyethoxy)ethanoyl)-1,3-propanediamine (30)—**Diol **29** (0.56g, 2 mmol) was co-evaporated with dry pyridine (3 × 10 mL), dissolved in dry pyridine (15 mL) and after cooling to 0 °C, 4, 4′-dimethoxytrityl chloride (0.81 g, 2.4 mmol) in CH_2Cl_2 was added dropwise slowly. The flask was removed from the ice and the reaction mixture stirred overnight, quenched with methanol (0.5 mL) and diluted with CH_2Cl_2 (50 mL). The mixture was washed with 5% $NaHCO_3$ (50 mL × 2), brine (50 mL) and dried over anhydrous sodium sulfate. The solution was concentrated in vacuo and the crude product was purified by silica gel chromatography (0–5% MeOH/CH_2Cl_2 containing 1% Et_3N). The appropriate fractions were combined, evaporated and dried in vacuum to give **30** as a yellow foam (0.12g, %), R_f 0.60 (8% MeOH/CH_2Cl_2). ^{1}H NMR (500 MHz, DMSO-d_6, δ, ppm): 7.85 (t, 1H, J= 6 Hz), 7.74 (t, 1H, J = 6 Hz), 7.38–7.39 (m, 2H), 7.31 (t, 2H, J = 7.5 Hz), 7.22–7.26 (m, 5H), 6.89 (d, 4H, J = 9 Hz), 4.76 (t, 1H, J = 5Hz), 3.91 (s, 2H), 3.85 (s, 2H), 3.73 (s, 6H), 3.63 (t, 2H, J = 5 Hz), 3.53 (t, 2H, J= 5 Hz), 3.47 (t, 2H, J = 5 Hz), 3.08–3.14 (m, 6H), 1.54 (p, 2H, J = 6.5 Hz). ^{13}C NMR (125.76 MHz, DMSO-d_6, δ, ppm): 29.37, 35.52, 35.61, 54.96, 59.99, 62.55, 69.92, 70.15, 70.22, 72.78, 85.45, 112.70, 113.11, 123.79, 126.57, 127.63, 127.71, 128.82, 129.57, 135.64, 135.99, 144.82, 149.52, 158.01, 169.07, 169.22. HRMS (ESI, M+Na^+) Calcd. for $C_{32}H_{40}N_2NaO_8$ 603.2682, act. 603.2680.

***N*-(2-(2-O-(2-cyanoethyl-*N*, *N*-diisopropylphosphoramidite)ethoxy)ethanoyl)-*N′*-(2-(2-(4, 4′-dimethoxytrityloxy)ethoxy)ethanoyl)-1,3-propanediamine (31)—**30 (0.11g, 0.19 mmol) was co-evaporated with 10% anhydrous pyridine in CH_2Cl_2 (2 × 10 mL) then dissolved in anhydrous CH_2Cl_2 (10 mL). DIEA (0.1 mL, 0.76 mmol) was added with stirring under argon followed by the addition of 2-cyanoethyl diisopropylchlorophosphoramidite (0.11 ml, 0.47 mmol). The mixture was stirred at room temperature for 2 hours with TLC monitoring (10 % MeOH/ethyl acetate, 1% Et_3N). The reaction was quenched with 4 drops anhydrous methanol and 20 mL CH_2Cl_2 was added. The reaction mixture was transferred to a dry 125 mL separatory funnel and washed quickly with 5% $NaHCO_3$ (10 mL × 2) and brine (10 mL). The organic layer was dried over anhydrous sodium sulfate and concentrated under reduced pressure. The residue was purified by silica gel flash chromatography (0–5% MeOH/ethyl acetate, 1% Et_3N). The appropriate fractions were combined, evaporated and dried in vacuum to give product as a pale yellow oil (0.12g, 81%), ^{31}P NMR (202.46 MHz, DMSO-d_6, δ, ppm): 148.68 (referenced to external 85% H_3PO_4).

Spacers 2, 14, 32, 33, and 34—The synthetic procedures for these spacers have been published. (10)

Thermal melting measurements

Absorbance vs. temperature (melting and annealing curves) profiles of the oligonucleotides were carried out in Teflon-capped 1-cm path length quartz cells under a nitrogen atmosphere using a Cary 3 Bio UV-visible spectrophotometer with a 6 × 6 multicell block Peltier and a temperature controller. Oligonucleotides were dissolved in 1.0 M NaCl, 10 mM Na_2HPO_4,

0.1 mM Na_2EDTA, pH 7 degassed buffer and were prepared in three concentrations: 1 μM, 5μM and 15 μM. Samples were covered with a layer of silicone oil and denatured by raising the temperature to 85° C for 10 min prior to an experiment. Melting and annealing experiments were conducted in two stages by starting the experiment at 85° C and cooling to 5° C and heating from 5° C and ending at 85° C. Absorbance was measured at 260 nm and the heating rate/cooling rate as 0.3° C/min with data collection at 0.2° C intervals. The absorbance vs. temperature data obtained on the Cary 3 spectrometer were exported in ASCII format to the software application Microcal Origin. The data were normalized to produce relative absorbance values and sigmoidal curves were obtained using Boltzmann logged data-fit function. First derivative of the melting curve was obtained from the above sigmoidal curve and then fitted with a Gaussian function to identify the center of the peak, which is the T_m or melting temperature.

RESULTS AND DISCUSSION

Spacer Design

A series of four spacers each containing two amide groups (shown as the parent diols **8**, **14**, **18**, and **22** in Figure 1.B.) was designed based on three criteria. First, the spacers in fully extended conformations had terminal oxygen atoms separated by 14.6 to 17.3 Å. The distances were chosen to lie within the middle of the range observed in crystal and NMR structures between the terminal 3′O and 5′-O of B-DNA duplexes. We checked these distances by downloading a series of PDB format files of B-DNA NMR and X-Ray structures from the Protein Data Bank of the Research Collaboratory for Structural Bioinformatics (RCSB). These were displayed in the molecular modeling program Sybyl (Tripos Inc.), wherein the distance between the terminal 3′-O and 5′-O of 17 B-DNA molecules was found to vary between 13.8 and 18.8 Å. The average distance between the 3′-O and 5′-O of a B-DNA duplex is 16.2 Å. The number of atoms (shortest direct path of connectivity) and the distance between the terminal oxygen atoms is shown for each spacer in Figure 1. This distance provides a rough guide for design; the actual distance would be expected to vary in order for the endcap to accommodate the geometry of the terminal base pair. Second, the series of spacers provides variation in the placement of the carboxamide groups over the top of the terminal bases. Direct contact appears to exist between the glycine carboxamide group and the template base in the closed form of Taq DNA polymerase (15,16), but there are too many variables to allow us to design a spacer that would provide exactly the observed contact geometry. Third, the linkers and their DMT protected monophopshoramidites were easy and inexpensive to synthesize and could be incorporated into synthetic oligonucleotides on automated synthesizers with conventional reagents and conditions.

For comparison to previously studied endcaps, this study included hexaethylene glycol (**25**), the napthalenetetracarboxylate dimides **26–28**, and a tetrathymidine loop. In addition, we prepared the terthiophene spacer **2**, which provided an opportunity to study and compare an exceptionally hydrophobic endcap. Several research groups had reported that hydrophobic, aromatic molecules such as naphthalene diimides **32–34** (3,12,17), *N*,*N*-dimethylstilbene dicarboxamide (8), trimethoxystilbenes(18) and stilbene ether (9) stabilized DNA duplexes through stacking interactions with the DNA bases. We expected that endcap 2, with a terthiophene core, would also have significant stacking interactions with the base pairs in a DNA duplex. The hydrophilic endcaps **8**, **14**, **18**, **22** more closely resemble the hexaethylene glycol linker (**25**) in hydrophilicity.

The strategy for synthesis of each of the spacers as a symmetrical diol is illustrated in Scheme 1. Diol **2** could be obtained in good yield by reaction of the dilithium salt of terthiophene with two equivalents of oxetane (10). Diols **8** and **14** were obtained by reaction

of the *O-t*-butyldimethylsilyl ethers of ethanolamine and propanolamine with diglcolyl chloride, followed by removal of the silyl protecting group with ethanolic HCl. Details for the synthesis of diol **14** have been reported (10). Diols **18** and **22** were obtained more directly by the reaction of either γ-butyrolactone or δ-valerolactone with 1,3-propanediamine. Diol **29** was obtained by reaction of methyl bromoacetate with 2-benzyloxyethanol to form the benzyl protected methyl ester (**26**) which is converted to the carboxylic acid derivative for coupling with 1,3-propanediamine to form the benzyl protected diol **28**. Deprotection by catalytic hydrogenation with Pd/C catalyst gives diol **29** in good yield. The synthesis of diols **32**–**34** followed the procedure described by Pingle et al. (10) Each diol is symmetrical and could be synthesized as a mono-DMTr derivative by reaction with one equivalent of DMTr chloride. Yields are generally in the 35–50% range, which although low, was not limiting because of the ease with which one can produce large amounts of the diols. Separation of the monotritylated products from starting material and bis-tritylated side product by silica gel chromatorgraphy was facile in each case. The tritylated spacers were easily transformed to the corresponding phosphoramidites by conventional protocols and the 4, 4′-dimethoxytrityl protected phosphoramidite derivatives incorporated into the oligonucleotide on an automated DNA synthesizer in good yield as illustated in Figure 1A. The sequences synthesized for this study are included in Tables 2 and 3.

Thermal melting studies

Thermal melting studies were carried out on four-base-pair duplexes containing the nucleosides dA, T, dG, and dC and endcaps **14** and **18** (Table 2) and **2**, **8**, **22**, **25**, **29**, **32**, **33**, and **34** (Table 3). The thermal melting profile of all endcapped DNA duplexes at varied concentrations (1–15 μM) was a sigmoidal curve indicative of the formation of a hairpin and a concentration independent, unimolecular process. If the oligonucleotides were dimerizing rather than forming hairpin stuctures, one would expect to see an increase in T_m values with an increase in concentration. In order to determine the endcaps preferences for specific base-pairs we examined one sequence, **IV**, in which the endcaps were stacked over an A•T base-pair and a second sequence, **V**, in which the endcaps were stacked over a C•G base-pair. With two of the endcaps, **14** and **18**, we included additional sequences in which the endcaps were placed over T•A (**I** and **III**) and G•C base-pairs (**II**).

The T_m values of the control sequences **i.-v.** (Table 1, no endcaps) were not determined. These sequences contain only two C•G (G•C) base-pairs and consequently would be expected to melt well below room temperature. Complementary 4-mers containing all C•G (G•C) base pairs have been reported to have T_m values ranging from 16.7 to 27.8°C. For comparison of relative stability we have tabulated the predicted free energies of association for complementary sequences **i.-v.** (Table 1), based on the unified parameters reported by SantaLucia (19). For purposes of comparison the free energy contribution from the end effect was included only for the corresponding uncapped end (compare to sequences in Table 2). From the calculated free energies of association, we might predict the relative order of the T_m values of the DNA duplexes of Table 1 to be **i** ≥ **v** > **iii** > **ii** ≥ **iv**. Deviation from this order in the corresponding endcap containing oligonucleotides would indicate base-specific association effects with the endcap.

The T_m values observed for sequences **I–V** containing endcaps **14** or **18** (Table 2), do not completely correlate with the predicted trend of the T_m values of unmodified DNA duplexes based on the calculated ΔG values in Table 1. The most stable duplex is **V**, in which the endcaps are positioned over a C•G base pair. Oligonucleotide **I** would be predicted to be slightly more stable based on the calculated free energies for association. Furthermore the T_m values for oligonucleotide **II** containing either endcap **14** or **18** are higher than the T_m values for oligonucleotide **III**, which is contrary to prediction. These results suggest that

there is a greater stabilization effect when the endcaps are adjacent to either a G•C or a C•G base pair. This observation is concordant with results reported by Benight and coworkers (20) from a study on hairpin DNA oligonucleotides. Stems with C•G base-pairs closing the loop show greater stability than stems in which the loop closing base-pair is A•T.

Because of the number of different endcaps we wished to investigate, other endcaps were incorporated only into sequences **IV** and **V**. This was sufficient to probe differences between the endcaps for stabilization of closing A•T versus C•G base pairs. As can be seen from the data all of the endcaps stabilize the four base-pair duplex, but the differences in stabilization are significant. Among the diamide aliphatic linkers, the degree of stabilization is related to the length. The shortest linker (**8**) is least stabilizing with T_m values for **IV** and **V** at 39 and 42 °C, while the longest (**22**) is most stabilizing, with T_m values for **IV** and **V** at 46 and 56 °C. Although **14**, **18**, and **22**, when fully extended, are all longer than the average distance of 16.2 Å observed for the 3′-O to 5′-O span between duplex ends in B-DNA, if the carbon-carbon bonds adjacent to these oxygens are in a gauche conformation rather than an antiperiplanar conformation, the lengths shorten by 1.6 to 2.9Å. For example, linkers **14** and **18**, which are both near the optimum length at 16.8 and 17.3 Å respectively, both show distances of 14.5 Å in a minimized structure in which the two terminal C-C bonds are gauche. Linker **8** (14.6 Å fully extended) spans only 11.4 Å in a minimized gauche conformation, while the longest linker, **22**, which is 19.5 Å fully extended falls to 17.9Å. The X-ray crystal structure for bis(2-hydroxyethyl)-stilbene-4,4′-diether linker capping a six base-pair stem (13) clearly shows that the terminal – OCH_2CH_2O- exist in the gauche-form. In modeling studies of the bridged duplexes the 3′-O to 5′-O distances were found to be 11.3, 14.7, 17.1 and 19.9 Å, for **8**, **14**, **18**, and **22** respectively. These models are interesting because each linker shows its own particular pattern of conformational preferences, but the gauche-form is noticeably absent from the carbon bonds adjacent to the phosphodiester group. In each of the structures, the 3′-endo (characteristic of B-DNA) conformation is maintained in all deoxyribose residues including those linked to the endcap.

Comparison to the hexaethylene glycol endcap (**25**) is instructive. This spacer is far longer (21.4 Å), but contains -OCH_2CH_2O- bonds for which the gauche conformation is favorable. The corresponding T_m values for oligonucleotides **IV** and **V** are higher (50 and 61°C) than for any of the amide containing endcaps. As a consequence it is not possible to say whether or not the amide groups provide any degree of stabilization through direct interactions with the face of the terminal base pair. It may be that the penalty for adopting higher energy conformations in order to fit between the 3′-O and 5′-O base-pair negates any advantage of amide-heterocycle interactions. Finally, we modified linker **22** by replacing two carbon atoms by oxygen atoms to create an analog in which the two terminals now contain the -OCH_2CH_2O- group (linker**29**). Presumably this analog, like **25** could more readily adopt a gauche conformation. In fact, the resulting T_m values (Table 3) were almost identical to those measured for compound **22**. It is possible that the increased flexibility was compromised by too short of a spacer distance with both terminal –OCH_2CH_2O- groups in a gauche conformation.

Stabilization by endcaps is greatest when aromatic residues capable of stacking interactions are included as part of the structure (3,8,13). For comparison we have included two types of aromatic moiety containing endcaps in these studies. The naphthalene tetracarboxylic acid diimide linker was studied previously by Bevers et al.(3), however, they used a -$OCH_2CH_2OCH_2CH_2$- spacer between the phosphodiester groups and the imide nitrogen atoms, whereas we used -$(CH_2)_3$-, -$(CH_2)_4$-, and -$(CH_2)_5$-spacers (**32**, **33**, and **34** respectively) in our studies. Both Bevers et al. with the naphthalendicarboxamide linkers and Lewis and coworkers (9) in the case of the stilbene linkers included -OCH_2CH_2O- spacers as part of the structure. Interestingly, the lack of this spacer in our linkers does not

appear to have compromised stability in all cases. One of these linkers (**34**) is nearly identical to the Bevers et al. linker. The difference is that we used $OCH_2CH_2CH_2CH_2CH_2$- in place of -$OCH_2CH_2OCH_2CH_2$-. Also, we measured T_m values in much shorter oligonucleotides sequences (ATGC-**34**-GCAT, T_m = 74° and GCTA-**34**-TAGC, T_m = 60° versus TCTTTTCTT-Y-AGAAAAGAA, T_m= 72°). Despite the shorter oligonucleotides, we obtained a higher T_m value when the naphthalene tetracarboxylate diimide was stacked over the C•G base pair. Our observed T_m value is significantly lower when the naphthalene was stacked over the A•T base pair. In the Bevers sequence the naphthalene is adjacent to a T•A base pair. It is likely that the Bevers linker would have caused a similar increase in stabilization when placed over a G•C or C•G base pair. Nevertheless, based on our high T_m values it does not appear likely that the absence of an -OCH_2CH_2O-spacer in our linker significantly compromised the stability. Furthermore the C3 spacer (in linker **32**), which would presumably be far too short based on our earlier analysis (16.0 Å fully extended), is the most stabilizing.

The hydrophobic terthiophene endcap **2** stabilized oligonucleotide **IV** (T_m = 66°C) to a greater extent than oligonucleotide **V** (T_m = 62 °C). This difference is particulary profound because non-bridged duplex **V** is considerably more stable than duplex **IV**. (Table 1). This presumably results from the greater hydrophobicity of the A•T base pair versus the C•G base pair.

Conclusions

This study confirms that endcaps containing conjugated aromatic π-systems, capable of base stacking, stabilize a short oligonucleotide duplex significantly more than endcaps containing other types of functionality. Moreover, we have now demonstrated that a highly hydrophobic endcap (**2**), enhances the stablity of a duplex to a greater extent when positioned over an A•T base pair than when stacked over a C•G base pair. The more hydrophilic naphthalene tetracarboxylate diimide stabilizes a duplex to a much greater extent when stacked over a C•G base pair.

The significantly greater stabilization of the 4 base-pair stems by a hexaethylene glycol in comparison to the four diamide containing aliphatic endcaps included in this study, suggests that greater spacer flexibility may allow the terminal base pair to achieve optimal conformation. Our results further support the contribution of π-stacking interactions in duplex stabilization by endcaps, as well as the importance of spacer structure linking the aromatic residue to the oligonucleotides phosphodiester groups.

An important goal of this research was to find spacers that would not alter the duplex in a way that would either hinder binding, or prevent readjustment of the structure as dictated by a protein binding to the dsDNA. Based on the T_m studies and taking into account spacer length, spacer **18** was incorporated into sequence IX (Figure 2). The spacer made it possible to create a single sequence (IX) that would take the place of three separate oligonucleotides (GCTAACC (VI), GGTIA (VII), and GC (VIII) required for the co-crystallization of the enzyme Endo V with its substrate, a nicked DNA. Sequences VII and VIII do not hybridize to the heptamer VI because VIII is too short (dimer) and VII contains an inosine mismatch. However, as illustrated in Figure 3 sequence is able to assume a duplex structure that in the presence of Endo V, can flip out the inosine nucleotide. Details of the Endo V structure and its interaction with sequence IX will be reported in a separate manuscript.

Supplementary Material

Refer to Web version on PubMed Central for supplementary material.

Acknowledgments

This work was supported by NASA under award NCC 2-1363, a grant from the National Institutes of Health (1R21EB006308), the National Science Foundation (0554990), the Indiana Elks Foundation and Walther Cancer Institute. Assistance from the National Cancer Institute Grant (P30 CA23168) awarded to Purdue University is also gratefully acknowledged. A Purdue Doctoral Fellowship provided support for Brian Laing.

References

1. Kool ET. Preorganization of DNA: Design Principles for Improving Nucleic Acid Recognition by Synthetic Oligonucleotides. Chemical Reviews. 1997; 97:1473–1488. [PubMed: 11851456]
2. Altmann S, Labhardt AM, Bur D, Lehmann C, Bannwarth W, Wüthrich K, Leupin W. NMR studies of DNA duplexes singly cross-linked by different synthetic linkers. Nucleic Acids Research. 1995; 23:4827–4835. [PubMed: 8532525]
3. Bevers S, O'Dea TP, McLaughlin LW. Perylene- and Naphthalene-Based Linkers for Duplex and Triplex Stabilization. Journal of the American Chemical Society. 1998; 120:11004–11005.
4. Doktycz MJ, Paner TM, Benight AS. Studies of DNA Dumbbells. IV. Preparation and Melting of a DNA Dumbbell with the 16 Base-Pair Sequence 5′-GTATCCCTCTGGATAC-3′ Linked on the Ends by Dodecyl Chains. Biopolymers. 1993; 33:1765–1777. [PubMed: 8268405]
5. Durand M, Chevrie K, Chassignol M, Thuong NT, Maurizot JC. Circular dichroism studies of an oligonucleotide containing a hairpin loop made of a hexaethylene glycol chain: conformation and stability. Nucleic Acids Research. 1990; 18:6353–6359. [PubMed: 2243780]
6. Gao H, Chidambaram N, Chen BC, Pelham DE, Patel R, Yang M, Zhou L, Cook A, Cohen JS. Double-Stranded Cyclic Oligonucleotides with Non-Nucleotide Bridges. Bioconjugate Chemistry. 1994; 5:445–453. [PubMed: 7849075]
7. Glick GD. Design, Synthesis, and Analysis of Conformationally Constrained Nucleic Acids. Biopolymers (Nucleic Acid Sciences). 1998; 48:83–96. [PubMed: 9846126]
8. Letsinger RL, Wu TF. Use of a Stilbenedicarboxamide Bridge in Stabilizing, Monitoring, and Photochemically Altering Folded Conformations of Oligonucleotides. Journal of the American Chemical Society. 1995; 117:7323–7328.
9. Lewis FD, Wu Y, Liu X. Synthesis, Structure, and Photochemistry of Exceptionally Stable Synthetic DNA Hairpins with Stilbene Diether Linkers. Journal of the American Chemical Society. 2002; 124:12165–12173. [PubMed: 12371856]
10. Pingle MR, Ng PS, Xu X, Bergstrom DE. Synthesis of endcap dimethoxytrityl phosphoramidites for endcapped oligonucleotides. Curr Protoc Nucleic Acid Chem. 2003; Chapter 5(Unit 5.6)
11. Ng PS, Bergstrom DE. Protein-DNA footprinting by endcapped duplex oligodeoxyribonucleotides. Nucleic Acids Res. 2004; 32:e107. [PubMed: 15263063]
12. Bevers S, Schutte S, McLaughlin LW. Naphthalene-Perylene-Based Linkers for the Stabilizattion of Hairpin Triplexs. Journal of the American Chemical Society. 2000; 122:5905–5915.
13. Egli M, Tereshko V, Mushudov GN, Sanishivili R, Liu XY, Lewis FD. Face-to-face and edge-to-face pi-pi interactions in a synthetic DNA hairpin with a stilbenediether linker. Journal of the American Chemical Society. 2003; 125:10842–10849. [PubMed: 12952463]
14. Hariharan M, Zheng Y, Long H, Zeidan TA, Schatz GC, Vura-Weis J, Wasielewski MR, Zuo X, Tiede DM, Lewis FD. Hydrophobic Dimerization and Thermal Dissociation of Perylenediimide-Linked DNA Hairpins. Journal of the American Chemical Society. 2009; 131:5920–5929. [PubMed: 19382814]
15. Li Y, Waksman G. Crystal structures of a ddATP-, ddTTP-, ddCTP, and ddGTP-trapped ternary complex of Klentaq1: insights into nucleotide incorporation and selectivity. Protein Sci. 2001; 10:1225–1233. [PubMed: 11369861]
16. Paul N, Nashine VC, Hoops G, Zhang P, Zhou J, Bergstrom DE, Davisson VJ. DNA polymerase template interactions probed by degenerate isosteric nucleobase analogs. Chem Biol. 2003; 10:815–825. [PubMed: 14522052]
17. Ng PS, Pingle MR, Balasundarum G, Friedman A, Zu X, Bergstrom DE. Endcaps for stabilizing short DNA duplexes. Nucleosides Nucleotides Nucleic Acids. 2003; 22:1635–1637. [PubMed: 14565484]

18. Tuma J, Paulini R, Rojas Stutz JA, Richert C. How Much pi Stacking Do DNA Termini Seek? Solution Structure of a Self-Complementary DNA Hexamer with Trimethoxystilbenes Capping the Terminal Base Pairs. Biochemistry. 2004; 43:15680–15687. [PubMed: 15595824]

19. SantaLucia J. A unified view of polymer, dumbbell, and oligonucleotide DNA nearest-neighbor thermodynamics. Proceedings of the National Academy of Sciences, USA. 1998; 95:1460–1465.

20. Vallone PM, Paner TM, Hilario J, Lane MJ, Faldasz BD, Benight AS. Melting studies of short DNA hairpins: influence of loop sequence and adjoining base pair identity on hairpin thermodynamic stability. Biopolymers. 1999; 50:425–442. [PubMed: 10423551]

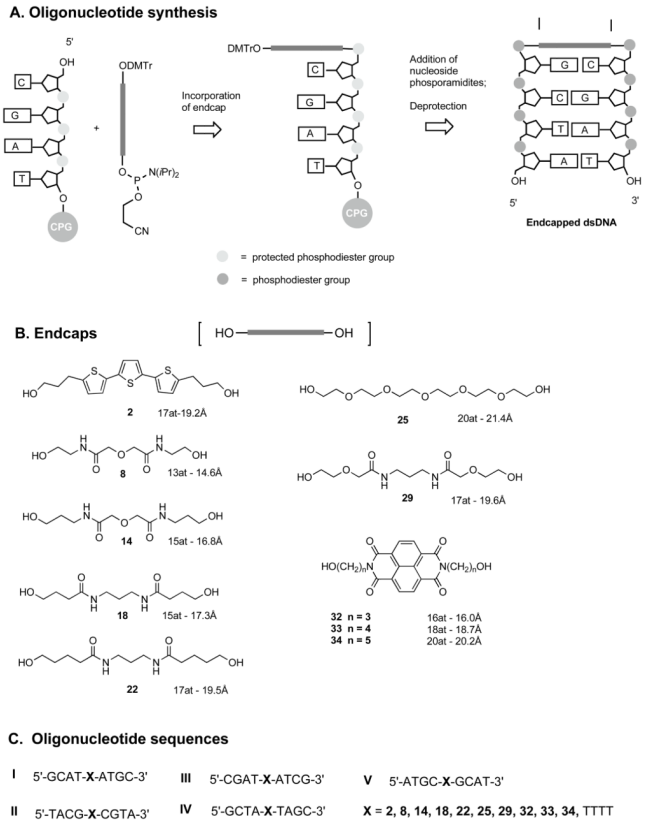

Figure 1.

Structure of endcapped DNA sequences. (A) Synthetic scheme for the incorporation of endcaps into oligonucleotides sequences. (B) Structures of endcaps used in this study (C) Tetramer oligonucleotides sequences.

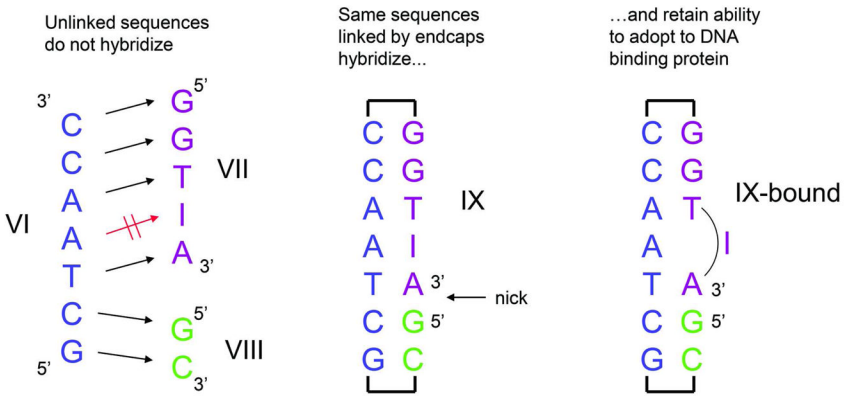

Figure 2.

Oligonucleotides VII and VIII do not form a stable hybrid duplex with oligonucleotide VI; Combination of the same nucleotide sequences with endcap **18** linking VIII and VII to VI gives duplex IX, which can be co-crystallized with Endo V to give the structure shown in Figure 3.

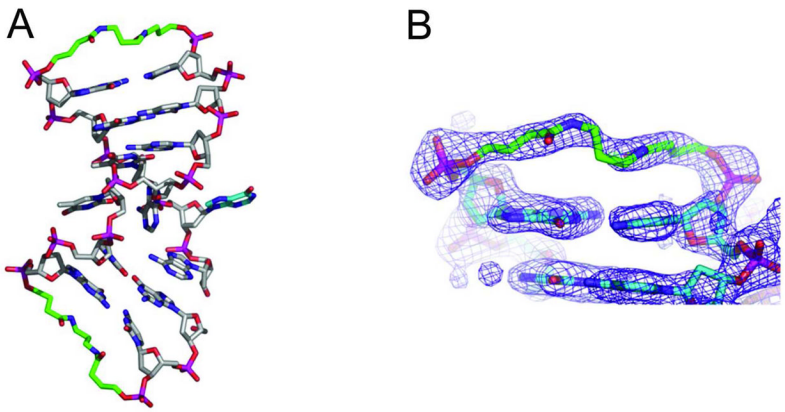

Figure 3.
Structure of oligonucleotide IX bound to Endo V (protein not shown).
A) Complete structure; B) Details of endcap **18**.

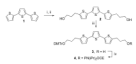

Scheme 1.

Synthetic pathway for the preparation of the phosphoramidite derivative of endcap **2**. **Reagents and conditions:** i. BuLi, −78°C; ii. $BF_3 \cdot Et_2O$, oxetane; iii. DMTrCl, pyridine; iv. 2-cyanoethyl-*N, N*-diisopropyl-chlorophosphoramidite, diisopropylethylamine.

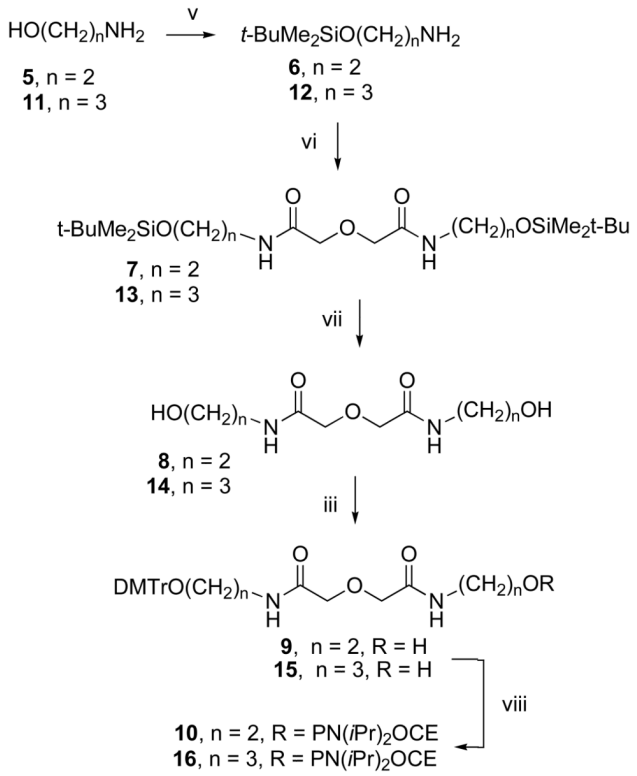

Scheme 2.

Synthetic pathway for the preparation of the phosphoramidite derivatives of endcaps **8** and **14**.

Reagents and conditions: iii. DMTrCl, pyridine; v. *t*BuMe$_2$SiCl, *N*,*N*-dimethylaminopyridine (DMAP), Et$_3$N; vi. diglycolyl chloride, Et$_3$N; vii. HCl, EtOH; viii. 2-cyanoethyl-*N*, *N*, *N*′, *N*′-tetraisopropylphosphorodiamidite, tetrazole.

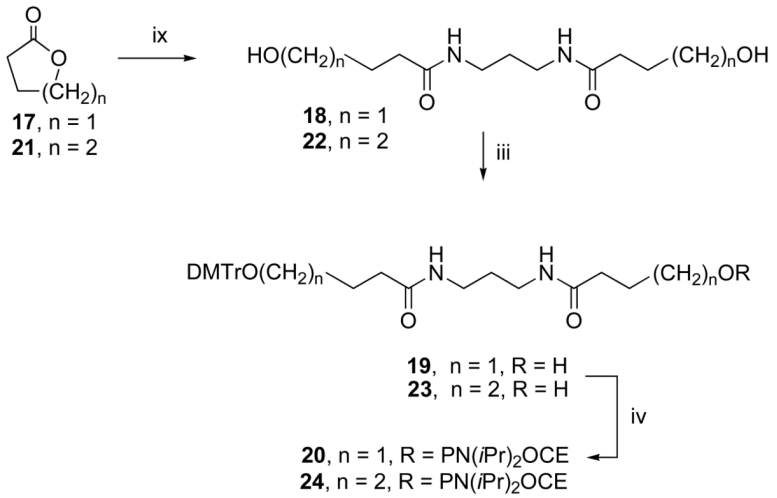

Scheme 3.

Synthetic pathway for the preparation of the phosphoramidite derivatives of endcaps **18** and **22**.

Reagents and conditions: iii. DMTrCl, pyridine; iv. 2-cyanoethyl-*N*, *N*-diisopropyl-chlorophosphoramidite, diisopropylethylamine; ix. 1,3-diaminopropane, DMAP, methanol.

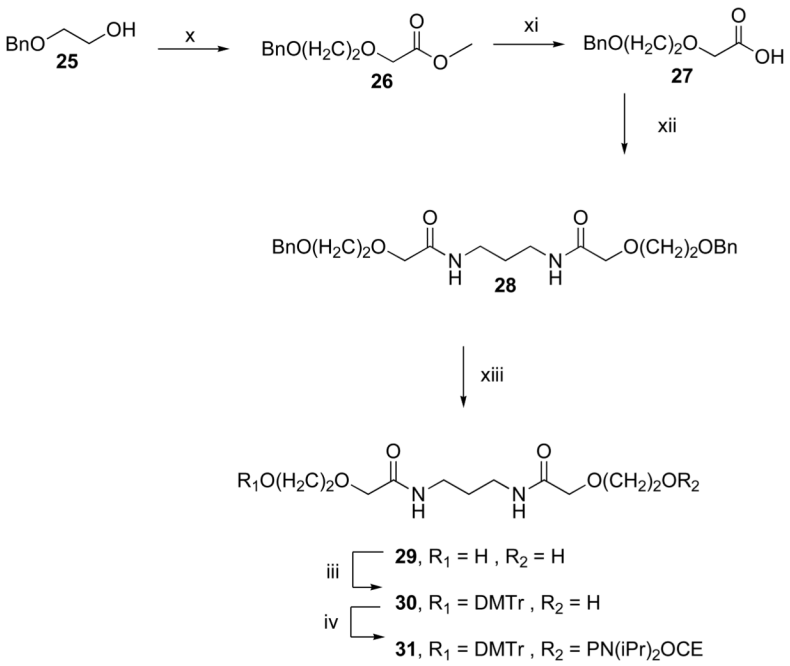

Scheme 4.

Synthetic pathway for the preparation of the phosphoramidite derivative of endcap **29**. **Reagents and conditions:** iii. DMTrCl, pyridine; iv. 2-cyanoethyl-*N*, *N*-diisopropyl-chlorophosphoramidite, diisopropylethylamine; x. methyl bromoactetate, NaH, THF reflux, r.t.; xi. MeOH, KOH, 35 °C; xii. 1,3 diaminopropane, TBTU, r.t.; xiii. H_2, Pd/C.

Table 1

Calculated Free Energy of Change for Association of Complementary Unmodified Tetramers

DNA sequences (5′→3′)	−ΔG (kcal/mol)
i. GCAT/ATGC	3.59
ii. TACG/CGTA	3.16
iii. CGAT/ATCG	3.37
iv. GCTA/TAGC	3.12
v. ATGC/GCAT	3.54

All DNA sequences are written in the 5′→3′ direction. The free energy factor for end effects was added only for the end opposite that covalently linked by endcaps (see oligonucleotides **I–V**, Table 2).

Table 2

T_m Values of Oligonucleotides **I–V** containing **14** & **18**

Oligonucleotide	Endcap T_{mb} values (°C)	
	14	**18**
I GCATXATGC	48	53
II TACGXCGTA	45	50
III CGATXATCG	44	48
IV GCTAXTAGC	41	44
V ATGCXGCAT	51	56

All DNA sequences are written in 5′→3′ direction. X: endcap

Table 3

T_m Values of Oligonucleotides **IV** & **V** containing **2, 8, 22, 29, 32–34** & TTTT

Oligonucleotide	**Endcap T_m values (°C)**								
	2	**8**	**22**	**25**	**29**	**32**	**33**	**34**	**TTTT**
IV	66	39	46	50	48	62	53	60	39
V	62	42	56	61	56	75	66	74	58

All DNA sequences are written in 5′→3′ direction. X: endcap

Bioconjug Chem. Author manuscript; available in PMC 2011 August 18.